

THE SUPERNOVAE INTEGRAL FIELD SPECTROGRAPH : KEYS TO HIGH-PRECISION SPECTRO-PHOTOMETRY.

C. Buton¹, on behalf of the Nearby Supernova Factory, Y. Copin¹, E. Gangler¹, G. Smadja¹, E. Pecontal², G. Rigaudier², P. Antilogus³, S. Bailey³, R. Pain³, R. Pereira³, C. Wu³, G. Aldering⁴, C. Aragon⁴, S. Bongard⁴, M. Childress⁴, S. Loken⁴, P. Nugent⁴, S. Perlmutter⁴, K. Runge⁴, R. C. Thomas⁴, B. A. Weaver⁴, C. Baltay⁵, A. Bauer⁵, D. Rabinowitz⁵ and R. Scalzo⁵

Abstract.

The Nearby Supernova Factory aims at discovering and observing a sample of type Ia supernovae through the dedicated Supernovae Integral Field Spectrograph, currently in operation since 2004 on Mauna-Kea UH telescope. To reach the targeted spectro-photometric accuracy, attention has been focused on various aspects of the calibration procedure, including: estimate of the night photometricity, derivation of the mean atmospheric extinction over the extended optical domain (320-1000 nm), its modeling in terms of physical components (Rayleigh and aerosol scatterings, ozone absorption and telluric lines) and its variability within a given night. Point-source extraction from the IFS datacube also requires a detailed knowledge of the atmospheric-induced point spread function (PSF). The overall accuracy of the calibration chain is estimated on reference flux standard stars.

1 Introduction

The Nearby Supernova Factory (SNfactory, Aldering et al. 2002) is an international project dedicated to the study of the nearby thermonuclear supernovae. Based upon the NEAT search for the target discovery and the dedicated 3D-spectrograph SNIFS for the follow up, the goal is to study the evolution of a vast sample of SNe Ia at $0.03 < z < 0.08$ from -15 to $+50$ days on the extended optical range (320 – 1000 nm). This will allow to probe in detail the local Hubble diagram, the SNe Ia physics, the SNe host galaxy correlations, etc.

The dedicated Supernova Integral Field Spectrograph (SNIFS, Lantz et al. 2004) mounted on the UH 2.2m telescope (Mauna Kea) comprises an IFS covering a $6'' \times 6''$ field from 300 to 1000 nm (blue and red channels with micro lens array), a photometric channel, covering $4' \times 5'$ around the IFS (monitoring of the atmospheric transmission) and an integrated guiding and focusing channel.

This contribution describes two steps of the calibration chain (Copin et al. 2007): the correction for the atmospheric extinction, and an empirical derivation of the point spread function which is needed because the field is too small and one wants to extrapolate the data to have a precise measurement of the flux.

2 Mean atmospheric extinction

In order to obtain the mean atmospheric extinction, one can break up the transmission of the atmosphere in this manner:

¹ Institut de physique nucléaire de Lyon, Université de Lyon, CNRS/IN2P3 UMR 5822, 4, rue E. Fermi 69622 Villeurbanne cedex, France

² Centre de Recherche Astronomique de Lyon, France

³ Laboratoire de Physique Nucleaire et de Haute Energies de Paris, France

⁴ Lawrence Berkeley National Laboratory, Berkeley, CA

⁵ Yale University, New Haven, CT

$$T_z(\lambda) = \frac{S(\lambda)}{S^*(\lambda) \times T(\lambda)} \quad (2.1)$$

where S is the observed spectrum, S^* the intrinsic spectrum, T the telescope transmission and T_z the atmospheric transmission.

To account for the various extinction components, T_z can be parametrised as:

$$T_z = 10^{-0.4K_Z} \text{ with } K_Z = \kappa(\lambda)z + \kappa_T(\lambda)z^\alpha \quad (2.2)$$

where $\kappa(\lambda)$ and $\kappa_T(\lambda)$ represent the different atmospheric extinction contributions which consists of four components (Adelman et al. 2003, see Fig. 1):

- Rayleigh scattering consists on a power law scattering by the air molecules (λ^{-4}).
- Ozone absorption which is concentrated to an altitude from 10 to 35 km . Two bands are to be considered, Huggins (UV) and Chapuis (visible), with two large peak of diffusion around 573 and 602 nm.
- Aerosol scattering is due to the particles and the various pollutants of human source discharged into the atmosphere (λ^α , $-1 < \alpha < 4$).
- Telluric lines (see Fig. 1) are absorption lines dues to O_2 and H_2O of the Earth atmosphere. The telluric correction is proportional to z^α ($0.5 < \alpha < 1$ for H_2O lines and $\alpha \simeq 0.5$ for O_2 saturated lines) (see Fig. 1).

As the telluric lines have a different behavior with respect to z , we need to treat in a separate way the correction of the extinction and the correction of the telluric lines (see Eq. 2.2).

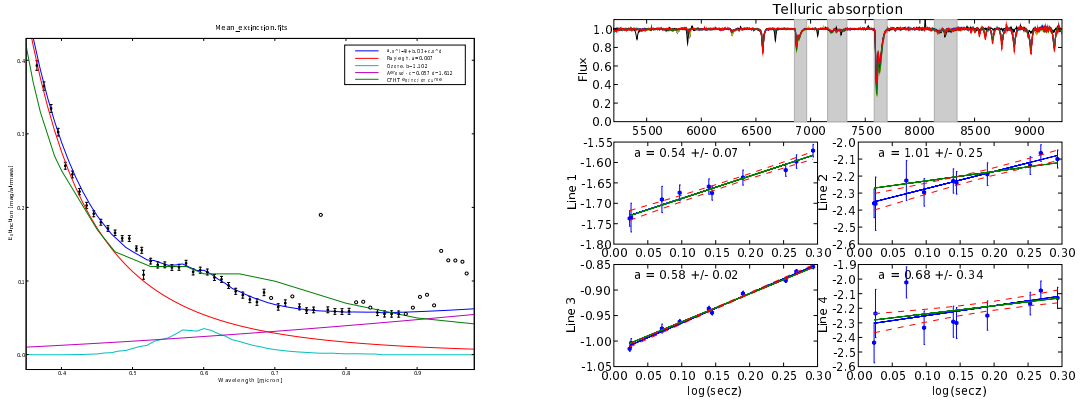


Fig. 1. Left: Computed SNIFS extinction (blue curve) in comparison with the original Mauna Kea extinction (green curve, Boulade O. 1987, Bèland et al. 1988); white points represent telluric lines, red curve represent Rayleigh component, blue curve represent ozone component and purple curve represent aerosol component. Right: Telluric exponent α for each telluric line computed from 10 stars of the night 06_014.

The function κ can be estimated from several exposures taken in the same night at different airmasses. Thus, Several κ allows to derive an average atmospheric extinction.

3 PSF radial profile

The point spread function (PSF) describes the response of an imaging system to a point source. For ground based optical telescopes, atmospheric turbulence (seeing) usually dominates the contribution to the PSF as it is the case for SNIFS.

The radial profile of the point spread function cannot be parametrised by a single gaussian function, a pair of gaussians, nor a Moffat function (Trujillo et al. 2001). It was found however that our data could be reproduced by the sum of a Gaussian for the core, and a Moffat function for the wings (see Fig. 2). An additional constant contribution is needed for the sky, as seen in equation 3.1:

$$PSF(r) = n_G \times \exp\left(\frac{r^2}{2\sigma^2}\right) + n_M \times \left(1 + \frac{r^2}{\alpha^2}\right)^{-\beta} + sky \quad (3.1)$$

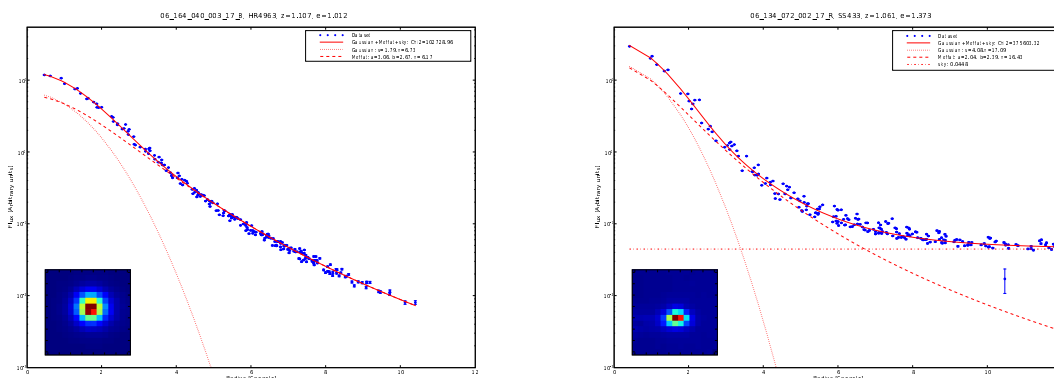


Fig. 2. Left: PSF radial profile fitted by a gaussian+moffat function for the short exposure star (~ 1 sec) HR4963. Right: same as left with a sky component for the long exposure (~ 300 sec) SS433.

To reduce the number of parameters involved, we have investigated their correlations with the radius α of the Moffat function. They are shown in Fig. 3 for a sample of 330 stars.

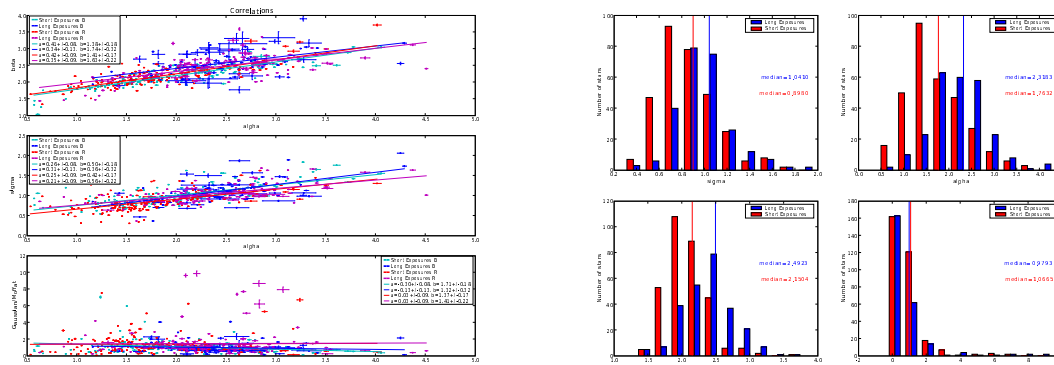


Fig. 3. Correlations and distributions of parameters for 330 stars observed by the SNFactory collaboration in 2006 (0 correlations fixed). The correlation parameters are different for long and short exposures but are the same for red and blue channel.

It is seen in Fig. 4 that when these correlations are imposed as linear relations, we are left with three free parameters in Eq. 3.2 (sky, α and N).

$$PSF(r) = N \times \eta(\alpha) \times \exp\left(\frac{r^2}{2\sigma(\alpha)^2}\right) + N \times \left(1 + \frac{r^2}{\alpha^2}\right)^{-\beta(\alpha)} + sky \quad (3.2)$$

where $\eta(\alpha) = \frac{\text{Gaussian norm}}{\text{Moffat norm}}$.

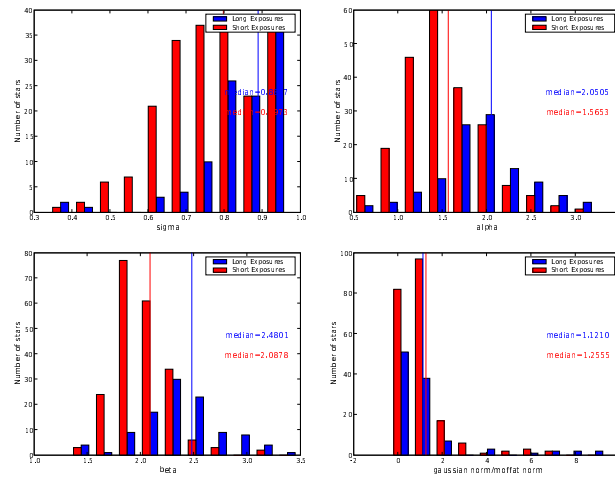


Fig. 4. distribution of the parameters for a sample of data truncated by $\sigma < 1.0$. It is interesting to point out that the parameter beta for the short exposures is significantly smaller than for the long exposures (Short N. et al. 2003).

After having imposed the correlations of σ , β and η with alpha, we obtain 'constrained' distributions for these parameters. It is observed in particular that in the sample with good seeing ($\sigma < 1''$, β parameter is especially well measured with good seeing), the parameter beta is significantly smaller for the short exposures (see Fig.4). A dependence of the power law on the exposure time is indeed expected from the work of Nicholas Short (Short et al. 2003).

4 Conclusion

We have measured with the SNIFS instrument of the SNfactory collaboration an accurate extinction curve at Mauna Kea, and derived a correction for telluric lines. These are important steps in the calibration chain of the SNfactory collaboration. Starting from preliminary studies, a good empirical description of the PSF was found, which can be used in the Point Source Extractor of the collaboration.

References

- Trujillo, I., Aguerri, J. A. L., Cepa, J., & Gutiérrez, C. M. 2001, The effects of seeing on Sérsic profiles -II. The Moffat PSF, *mnras*, 328, 977
- Aldering, G. et al. 2002, Overview of the Nearby Supernova Factory, in *Survey and Other Telescope Technologies and Discoveries*, ed. Tyson, J. A.; Wolff, S. Proceedings of the SPIE, 4836, 61
- Copin, Y. et al. 2007, this volume
- Adelman, S. et al. 2003, Round table on instrumentation and data processing, *Modelling of stellar atmospheres*, Astronomical Society of the Pacific, 210, 337
- Lantz, B. et al. 2004, SNIFS: a wideband integral field spectrograph with microlens arrays, in *Optical Design and Engineering*, ed. Mazuray, L., Rogers, P. J.; Wartmann, R. Proceedings of the SPIE, 5249, 146
- Bèland, S., Boulade, O., & Davidge, T. 1988, *Bulletin d'information du telescope Canada-France-Hawaii*, 19, 16
- Boulade, O. 1987, *Bulletin d'information du telescope Canada-France-Hawaii*, 17, 13
- Cuillandre, J.-C. et al. 2002, CFHT's SkyProbe: a real-time sky-transparency monitor, in *Observatory Operations to Optimize Scientific Return III*, ed. Quinn, P. J. Proceedings of the SPIE, 4844, 501
- Short N., Fitetson W., Hale D., Townes C. 2003, *Interferometry for optical astronomy*, Proceedings of SPIE Vol. 4838(2003).